Potentiation of large conductance, Ca^{2+}-activated K^+ (BK) channels by $\alpha5\beta1$ integrin activation in arteriolar smooth muscle

Xin Wu[2], Yan Yang[1], Peichun Gui[1], Yoshiro Sohma[3], Gerald A. Meininger[1], George E. Davis[1], Andrew P. Braun[4] and Michael J. Davis[1]

[1]*Department of Medical Pharmacology & Physiology and Dalton Cardiovascular Research Center, University of Missouri School of Medicine, Columbia, MO 65212, USA*

[2]*Department of Systems Biology & Translational Medicine, Texas A&M Health Science Center, College Station, TX 77843, USA*

[3]*Department of Physiology, Osaka Medical College, Takatsuki, Osaka 569–8686, Japan*

[4]*Smooth Muscle Research Group, University of Calgary School of Medicine, Calgary, Alberta, Canada T2N 4 N1*

Injury/degradation of the extracellular matrix (ECM) is associated with vascular wall remodelling and impaired reactivity, a process in which altered ECM–integrin interactions play key roles. Previously, we found that peptides containing the RGD integrin-binding sequence produce sustained vasodilatation of rat skeletal muscle arterioles. Here, we tested the hypothesis that RGD ligands work through $\alpha5\beta1$ integrin to modulate the activity of large conductance, Ca^{2+}-activated K^+ (BK) channels in arteriolar smooth muscle. K^+ currents were recorded in single arteriolar myocytes using whole-cell and single-channel patch clamp methods. Activation of $\alpha5\beta1$ integrin by an appropriate, insoluble $\alpha5\beta1$ antibody resulted in a 30–50% increase in the amplitude of iberiotoxin (IBTX)-sensitive, whole-cell K^+ current. Current potentiation occurred 1–8 min after bead–antibody application to the cell surface. Similarly, the endogenous $\alpha5\beta1$ integrin ligand fibronectin (FN) potentiated IBTX-sensitive K^+ current by 26%. Current potentiation was blocked by the c-*Src* inhibitor PP2 but not by PP3 (0.1–1 μM). In cell-attached patches, number of open channels $\times$ open probability (NP_o) of a 230–250 pS K^+ channel was significantly increased after FN application locally to the external surface of cell-attached patches through the recording pipette. In excised, inside-out patches, the same method of FN application led to large, significant increases in NP_o and caused a leftward shift in the NP_o–voltage relationship at constant $[Ca^{2+}]$. PP2 (but not PP3) nearly abolished the effect of FN on channel activity, suggesting that signalling between the integrin and channel involved an increase in Ca^{2+}sensitivity of the channel via a membrane-delimited pathway. The effects of $\alpha5\beta1$ integrin activation on both whole-cell and single-channel BK currents could be reproduced in HEK 293 cells expressing the BK channel α-subunit. This is the first demonstration at the single-channel level that integrin signalling can regulate an ion channel. Our results show that $\alpha5\beta1$ integrin activation potentiates BK channel activity in vascular smooth muscle through both Ca^{2+}- and c-*Src*-dependent mechanisms. This mechanism is likely to play a role in the arteriolar dilatation and impaired vascular reactivity associated with ECM degradation.

(Received 6 December 2007; accepted after revision 23 January 2008; first published online 24 January 2008)
Corresponding author M. J. Davis: Department of Medical Pharmacology & Physiology, University of Missouri School of Medicine, 1 Hospital Dr, Rm M451, Columbia, MO 65212, USA. Email: davismj@health.missouri.edu

Integrins are heterodimeric transmembrane receptors (α, β) that mediate cell adhesion to the extracellular matrix (ECM). Integrin subunits have extracellular domains that bind ECM proteins and short cytoplasmic tails that lack intrinsic kinase activity but associate with a complex of focal adhesion proteins, including numerous tyrosine kinases. The complete activation of integrin-linked signalling pathways, including recruitment and tyrosine phosphorylation of downstream protein targets, requires both integrin receptor occupation and clustering through interactions with insoluble ECM ligands (Yamada *et al.* 1985; Clark & Brugge, 1995).

Our previous work has shown that peptides containing the RGD (Arg-Gly-Asp) sequence, which interact

 DOI: 10.1113/jphysiol.2007.149500

with $\alpha v\beta 3$, $\alpha 5\beta 1$ and other integrins, produce acute constriction of isolated skeletal muscle arterioles. Constriction is followed by a sustained, dose-dependent vasodilatation (Mogford *et al.* 1996, 1997). The constriction is partly explained by signalling between $\alpha 5\beta 1$ integrin and the L-type Ca^{2+} channel in arteriolar smooth muscle (Wu *et al.* 1998, 2001), through a tyrosine kinase cascade in which focal adhesion kinase and c-*Src* play critical roles (Wu *et al.* 2001; Gui *et al.* 2006). However, the mechanism of the secondary, sustained vasodilatation remains unexplained; the observation that it is blocked by K^+ channel antagonists (Platts *et al.* 1998) suggests the involvement of one or more K^+ channels.

Studies show that at least two of the major K^+ channels in vascular smooth muscle (VSM) are regulated by protein tyrosine phosphorylation downstream from growth factor and/or integrin receptor signalling (Davis *et al.* 2001, 2002). hERG K^+ channels, which may contribute to the resting potential of visceral smooth muscle (Akbarali *et al.* 1999), are known to be activated in some cell types (Hofmann *et al.* 2001) following adhesion to the endogenous $\alpha 5\beta 1$ integrin ligand fibronectin (FN). Likewise, Ca^{2+}-activated K^+ channels in erythroleukaemia cells are activated following cell contact with insoluble FN, which is known to engage and aggregate several $\beta 1$ and $\beta 3$ integrins. The downstream effect of integrin activation in that system is an increase in whole-cell, Ca^{2+}-activated K^+ current leading to membrane hyperpolarization (Arcangeli *et al.* 1991, 1993; Becchetti *et al.* 1992). These observations support a possible signalling mechanism between $\beta 1/\beta 3$ integrins and Ca^{2+}-activated K^+ channels.

Large-conductance Ca^{2+}-activated K^+ (BK) channels are highly expressed in VSM and function, at least in part, to counteract depolarizing stimuli that activate Ca^{2+} channels (Brayden & Nelson, 1992). The BK channel is composed of a pore-forming α-subunit and accessory β-subunit (Toro *et al.* 1998) and is activated both by depolarization and by increases in local Ca^{2+} concentration (Nelson & Quayle, 1995; Jackson & Blair, 1998). BK channels are known to undergo protein phosphorylation by intracellular kinases, including c-*Src*, resulting in shifts in the apparent Ca^{2+} sensitivity of the channel (Toro *et al.* 1998; Brenner *et al.* 2000; Cox & Aldrich, 2000; Ling *et al.* 2000; Braun & Sy, 2001; Swayze & Braun, 2001; Alioua *et al.* 2002). For these reasons, we hypothesized that the BK channel may be a downstream target of integrin activation in VSM and may mediate part of the arteriolar vasodilatation produced by integrin ligands. The purpose of the present study was to determine if BK channels in arteriolar smooth muscle cells are regulated by $\alpha 5\beta 1$ integrin signalling.

Methods

Arteriolar smooth muscle cell isolation

Arteriolar myocytes from first- and second-order vessels were isolated according to the method of Wu *et al.* (Wu *et al.* 2001), with slight modifications. Male Sprague–Dawley rats (120–200 g) were anaesthetized with pentobarbital sodium (120 mg kg^{-1}, I.P.). All animal handling procedures followed institutional guidelines and were approved by animal care committees at the University of Missouri and Texas A&M University. Cremaster muscles were excised and pinned flat for vessel dissection at 4°C in Ca^{2+}-free physiological saline solution (PSS) containing (mM): 147 NaCl, 8.6 KCl, 1.17 $MgSO_4$, 1.2 NaH_2PO_4, 5.0 D-glucose, 2.0 pyruvate, 0.02 EDTA, 3 mM Mops, plus 0.1 mg ml^{-1} bovine serum albumin (BSA, Amersham Life Science, Arlington Heights, IL, USA). The animal was then killed with an overdose of pentobarbital (300 mg kg^{-1}, I.C.). Dissected segments of arterioles were transferred to a 1 ml tube of low-Ca^{2+} PSS containing (mM): 144 NaCl, 5.6 KCl, 0.1 $CaCl_2$, 1.0 $MgCl_2$, 0.42 Na_2HPO_4, 0.44 NaH_2PO_4, 10 Hepes, 4.17 $NaHCO_3$, and 1 mg ml^{-1} BSA at room temperature for 10 min. The solution was decanted and replaced with a similar solution containing 26 U ml^{-1} papain (Sigma, St Louis, MO, USA) and 1 mg ml^{-1} dithioerythritol. The vessels were incubated for 30 min at 37°C with occasional agitation, then transferred to a new tube containing low-Ca^{2+} PSS containing 1.95 U ml^{-1} collagenase (FALGPA, Sigma), 1 mg ml^{-1} soybean trypsin inhibitor (Sigma) and 75 U ml^{-1} elastase (Calbiochem, La Jolla, CA, USA), and incubated for 15 min at 37°C. After further digestion, the remaining fragments were gently rinsed 2–3 times with low-Ca^{2+} PSS without BSA and gently triturated using a fire-polished Pasteur pipette to release single cells. Spindle-shaped arteriolar myocytes were used within 4 h of isolation.

Electrophysiological recordings

Patch clamp techniques were employed using an EPC-9 amplifier (HEKA, Germany) to measure membrane current in the whole-cell, cell-attached and inside-out patch configurations (Hamill *et al.* 1981). The amplifier was controlled by a Dell XPS computer running Pulse + Pulsefit software through an ITC-16 interface (Instrutech, Port Washington, NY, USA). Igor Pro (WaveMetrics, Oswego, OR, USA) and Sigma Plot 9.0 (SPSS Inc., Ashburn, VA, USA) were used for data analysis. Micropipettes were pulled from borosilicate glass capillaries (Corning 8161; ID, 1.2 mm; OD, 1.5 mm; WPI, Sarasota, FL, USA) using a Sutter P-97 electrode puller (Sutter Instruments, Foster City, CA, USA).

For whole-cell recordings, pipette resistances ranged from 2.5 to 5.0 MΩ when filled with pipette solution.

Whole-cell K^+ currents were evoked by voltage steps delivered from a typical holding potential (V_h) of −60 mV to potentials ranging from −80 to +80 mV, in 10 mV increments, with a typical duration of 200 ms. Currents were sampled at 10 kHz and filtered at 3 or 5 kHz. BK currents were identified as the IBTX-sensitive component of total K^+ current.

For single-channel recordings, pipettes were 3–5 MΩ and were usually coated with beeswax to reduce noise from stray capacitance. Recordings were filtered at 1 kHz to further reduce noise. BK channels were identified from current–voltage (I–V) relationships obtained at different V_h values from −80 to +80 mV or with voltage ramps from −100 mV to +100 mV (1 s duration). All experiments were performed at room temperature.

Solutions

For whole-cell recordings, two sets of bath and pipette solutions were used. The 136 mM Na^+ bath solution contained (mM): 136 NaCl, 5.9 KCl, 1.8 $CaCl_2$, 1.2 $MgCl_2$, 18 glucose, 1.16 NaH_2PO_4, 10 Hepes, 0.02 EGTA and 2 sodium pyruvate (pH 7.4). The 140 mM Na^+ bath solution contained (mM): 140 NaCl, 5.4 KCl, 2 $CaCl_2$, 1 $MgCl_2$, 10 glucose, 10 Hepes, 2 sodium pyruvate (pH 7.4). The 115 mM K^+ pipette solution contained (mM): 6 NaCl, 115 KCl, 10 Hepes, 1.15 $NaPO_4$, 1.15 NaH_2PO_4, 1.18 $MgCl_2$, 11 glucose, 2 EGTA (pH 7.2); $CaCl_2$ was added to bring free $[Ca^{2+}] = 100$ nM. The 140 mM K^+ pipette solution contained (in mM): 140 KCl, 8 NaCl, 1–2 EGTA, 3 Mg-ATP, 10 Hepes (pH 7.2); $CaCl_2$ was added to bring free $[Ca^{2+}]$ to 600 nM. 4-aminopyridine (4-AP; 1 mM) and glibenclamide (500 nM) were added to the bath solution as indicated to block K_v and K_{ATP} channels, respectively. The addition of other reagents to the bath and/or pipette solutions for specific protocols is stated in the figure legends.

Chemicals

Paxilline was obtained from Transduction Laboratories (Lexington, KY, USA) and Alomone Laboratories (Jerusalem, Israel). Iberiotoxin (IBTX) was obtained from Alomone Laboratories and Sigma. Anti-rat $\alpha5$ integrin monoclonal antibody (HMα5-1), used for protocols on rat VSM cells, was obtained from Pharmingen (San Diego, CA, USA). Anti-rat MHC class I monoclonal antibody (major histocompatability complex; MHC) was obtained from Seikagaku Inc. (Tokyo, Japan). Anti-human $\alpha5\beta1$ integrin monoclonal antibody (JBS5), used for protocols on HEK cells, was obtained from Chemicon (Temecula, CA, USA). Soluble purified fibronectin (FN) fragment (120 kDa), RGD (Arg-Gly-Asp) peptide, PP2 and PP3 were obtained from Chemicon. The BK channel blocker tetraethylammonium chloride (TEA), the small-conductance Ca^{2+}-activated K^+ channel (SK) blocker apamin, the intermediate-conductance Ca^{2+}-activated K^+ channel (IK) blocker TRAM-34 and all other chemicals, except as specifically stated, were obtained from Sigma-Aldrich.

Application of reagents

Anti-$\alpha5$ integrin antibody was coated onto 3.2-μm-diameter streptavidin-coated microspheres (Bangs Laboratories, Fishers, IN, USA) using a biotinylation procedure and applied to individual cells using pressure ejection from a picospritzer micropipette, as previously described (Wu *et al.* 1998, 2001). Soluble RGD and FN were prepared as stock solutions by dissolving the lyophilized compounds in bath or pipette solution, followed by gentle mixing. IBTX, PP2 and PP3 were added to the bath solution.

m*Slo* expression in HEK 293 cells

HEK 293 cells (tsA-201 line) were maintained at 37°C in a 5% CO_2 incubator in Dulbecco's modified Eagle's medium (DMEM) containing L-glutamine, 4.5 g l^{-1} D-glucose and 10% (v/v) fetal bovine serum (Invitrogen, Carlsbad, CA, USA). Transient transfection of cells at 50–60% confluency was carried out in 35 mm tissue culture dishes using the lipofection technique. LipofectAMINE (6–8 μl) was mixed with 0.5 μg of total plasmid cDNA (0.2 μg GFP + 0.3 μg m*Slo*, or 0.2 μg GFP + 0.2 μg m*Slo* + 0.1 μg BK channel $\beta1$-subunit) in 1 ml of serum-free DMEM and placed on cells for 5–6 h at 37°C in a humidified incubator containing 5% CO_2. The cDNA-containing medium was then aspirated and replaced with 10% serum-containing medium. The following day, cells were detached using 0.025% trypsin–0.5 mM EDTA in phosphate-buffered saline and replated onto sterile glass coverslips coated with 0.0001% poly L-lysine in 35 mm culture dishes. Whole-cell current recordings were typically performed on days 2–4 following transfection.

Data analysis

For most whole-cell analyses, raw current values were normalized to cell capacitance and expressed as current density (pA pF^{-1}). For single-channel analysis, amplitude histograms were constructed from continuous recordings at constant V_h and fitted with Gaussian curves to determine average current amplitude. NP_o (number of open channels × open probability) was computed using the method and program previously described (Sohma *et al.* 1996). Summary data are expressed as mean ± S.E.M. Statistical significance was determined using t tests, paired

t tests, or ANOVA, as indicated for specific protocols. Significance levels of $P < 0.05$ were considered significant.

Results

Activation of $\alpha5\beta1$ integrin leads to potentiation of whole-cell BK current

In the whole-cell patch clamp configuration, voltage-dependent K^+ currents in single arteriolar myocytes were activated by depolarizing voltage steps (Fig. 1*A*). Based on previous experience with rat cremaster arteriolar myocytes (Wu *et al.* 2001), whole-cell K^+ currents were likely to be composed primarily of a combination of K_v and BK currents, because addition of 20 mM TEA to the bath or equimolar replacement of KCl with CsCl in pipette solution (140 mM) resulted in almost complete elimination of outward current ($n = 5$, data not shown). With 100 nM Ca^{2+} in the recording pipette and in the presence of 4-AP and glibenclamide externally, the majority of outward current was sensitive to the highly selective BK channel antagonist IBTX (100 nM), as shown by the representative traces (Fig. 1*A*, inset). Summary *I–V* curves from six cells in the absence and presence of IBTX

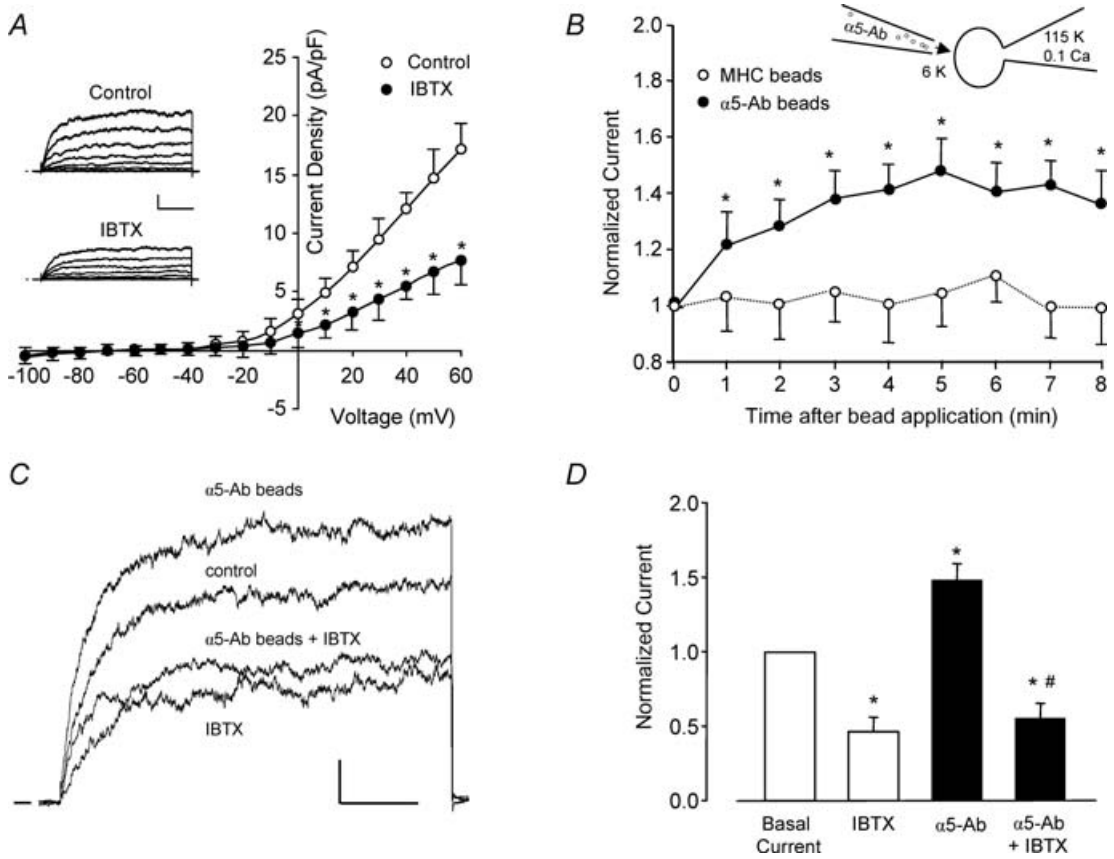

Figure 1. An outward, IBTX-sensitive K^+ current is enhanced by $\alpha5\beta1$ integrin activation
A, average outward current (expressed as current density, pA pF^{-1}) from freshly isolated rat cremaster muscle arteriolar myocytes is plotted as a function of voltage (test pulse), with or without 100 nM IBTX present in the bath ($n = 6$). Inset, representative whole-cell current traces from a single myocyte under control conditions and with 100 nM IBTX in the bath. Calibration bar: 100 pA, 50 ms. $V_h = -60$ mV. *B*, time course of K^+ current enhancement following $\alpha5\beta1$ integrin activation by beads coated with anti-rat $\alpha5$ integrin antibody (HMα5-1); beads were applied from a picospritzer pipette (~5 beads $cell^{-1}$). Beads coated with anti-rat MHC Class I Ab were used as a control to test for a mechanical artifact (○, $n = 7$). Inset shows the recording configuration for panels *B–D*, with the bath solution containing 6 mM K^+ and pipette solution containing 115 mM K^+ and 0.1 μM Ca^{2+}. *C*, sample recordings of whole-cell K^+ current from two arteriolar myocytes in the absence and presence of $\alpha5\beta1$ integrin activation and IBTX (100 nM). Holding potential = −60 mV, test potential = +50 mV, duration = 200 ms. $\alpha5\beta1$ integrin was activated by $\alpha5\beta1$ integrin Ab bound to beads (3 beads for this cell). In a second cell, the potentiation of current in response to integrin activation was blocked in the presence of IBTX (100 nM). Calibration bar: 100 pA, 50 ms. *D*, summary of effects of insoluble $\alpha5$-Ab on BK current in VSM in the absence ($n = 5$) or presence of IBTX ($n = 6$). Bath solution, 136 Na^+ + 4-AP (1 mM) + glibenclamide (500 nM); pipette, 115 K^+ (0.1 μM [Ca^{2+}]). *$P < 0.05$ *versus* control (basal current); #$P < 0.05$ *versus* $\alpha5$-integrin Ab.

are shown in Fig. 1*A*. IBTX inhibited, on average, ∼54% of whole-cell K^+ current, suggesting that this fraction of total K^+ current was contributed by BK channels. When a pipette solution containing a higher free $[Ca^{2+}]_i$ was used (600 nM), IBTX inhibited a larger fraction of the total K^+ current, ∼70% (not shown).

The application of microbeads coated with $\alpha5$ integrin antibody (HMα5-1-Ab) has been shown previously to activate $\alpha5\beta1$ integrin on rat cremaster arteriolar myocytes (Wu *et al.* 2001) and other cells (Yamada *et al.* 1985) through ligation and clustering of the integrin receptor. Under conditions optimal for recording K^+ current, the application of $\alpha5$-Ab-coated beads to individual myocytes resulted in potentiation of macroscopic outward current by ∼1.5-fold. The time course of K^+ current activation in response to +50 mV voltage clamp steps applied once per minute is shown in Fig. 1*B*. The full response was reached within 4–5 min. Current potentiation was not due to a non-specific mechanical effect because, in another group of cells, beads coated with a control Ab (rat MHC) had no significant effect. Sample recordings from two cells are shown in Fig. 1*C*, ∼5 min after $\alpha5$-Ab bead application, where K^+ currents were evoked by repeated voltage steps to +50 mV. In the first cell, current was potentiated by ∼30% after decoration of the cell with $\alpha5$-Ab-coated beads. In a second cell exhibiting approximately the same amount of K^+ current under control conditions (not shown), IBTX (100 nM) reduced basal current by ∼45%; the subsequent application of $\alpha5$ beads in the continued presence of IBTX failed to potentiate K^+ current. Figure 1*D* summarizes the effect of $\alpha5$-Ab bead application in the presence and absence of IBTX. On average, $\alpha5$-Ab bead application produced 48% potentiation of K^+ current and IBTX inhibited ∼54% of basal K^+ current. In the presence of IBTX, no significant potentiation of current occurred in response to $\alpha5$-Ab bead application.

Next, we tested other methods of activating $\alpha5\beta1$ integrin. In previous studies examining the effects of $\alpha5\beta1$ integrin ligands on L-type Ca^{2+} current, $\alpha5$-Ab-coated beads were found to cause a greater effect than the endogenous $\alpha5\beta1$ integrin ligand, FN (Wu *et al.* 1998). As shown in the recordings in Fig. 2*A*, exposure of a VSM cell to soluble FN (10 μg ml^{-1}; 120 kDa FN fragment), either via the bath or from a picospritzer pipette, potentiated whole-cell K^+ current by up to ∼80% at +80 mV (middle trace; time, 5 min; $[Ca^{2+}]_i \approx 600$ nM). Subsequent application of IBTX reduced current below control levels, as shown in the lower set of traces. It was not possible to test the effects of both IBTX and FN on each cell before and after reagent application because neither reagent could be completely washed out. The *I–V* relationship for the same cell is shown in Fig. 2*B*. The actions of FN and other $\alpha5\beta1$ integrin ligands are summarized in Fig. 2*C*. On average, FN potentiated macroscopic K^+ current by 26% ($[Ca^{2+}]_i \approx 100$ nM). Soluble $\alpha5\beta1$ Ab, which presumably ligates but does not crosslink and cluster $\alpha5\beta1$ integrins (Yamada *et al.* 1985), did not produce significant potentiation of K^+ current. RGD peptide potentiated current by 22%. Although the peptide was applied in soluble form, it may have interacted with both $\alpha5\beta1$ and $\alpha v\beta3$ integrins, the latter of which has been linked to the activation of BK channels in endothelium (Kawasaki *et al.* 2004). Also, RGD peptide is known to have agonist or antagonist activity depending on the dose (Tsao & Mousa, 1995). The hierarchy of responses, insoluble $\alpha5$ integrin Ab > FN > RGD, is consistent with the known affinities of $\alpha5\beta1$ integrin for the respective ligands. The control peptide (RAD), which does not ligate integrins (Silletti *et al.* 2000; Martinez-Lemus *et al.* 2005), was without a significant effect on K^+ current.

Our previous studies found that activation of $\alpha5\beta1$ integrin in VSM cells led to potentiation of Ca^{2+} current in part through activation of c-*Src* (Wu *et al.* 2001). Other studies have shown that the tyrosine kinase, c-*Src*, can phosphorylate the BK channel and lead to alterations in channel gating and/or Ca^{2+} sensitivity (Ling *et al.* 2000; Alioua *et al.* 2002). To test the possibility that the potentiation of the BK channel by $\alpha5\beta1$ integrin activation may involve c-*Src*, the soluble c-*Src* inhibitor PP2 (100 nM), was applied to the bath solution while recording whole-cell K^+ current. Under control conditions, PP2 caused ∼14% reduction in BK current amplitude and completely inhibited the potentiation of current following $\alpha5\beta1$ integrin activation (Fig. 2*D*). Application of the inactive analogue PP3 (100 nM) did not significantly reduce basal K^+ current or alter the amount of current potentiation induced by $\alpha5\beta1$ integrin activation.

Effect of $\alpha5\beta1$ integrin activation on single BK channel currents

Next, we investigated integrin-induced potentiation of BK current using single-channel recording methods. The activity of single BK channels was recorded either in cell-attached or excised, inside-out patches from freshly isolated arteriolar myocytes, with the cell or patch bathed in 140 mM K^+ solution to zero the membrane potential and equalize the K^+ gradient. The large single-channel conductance of BK channels was utilized as a marker of channel activity in our recordings and was confirmed using two separate methods: (1) Single-channel currents were recorded for several seconds at various membrane potentials between −80 and +80 mV, after which current amplitudes were detected using Pulse + Pulsefit and the average amplitudes of the events determined from Gaussian fits of the amplitude histogram (Sohma *et al.* 1996); (2) Alternatively, channel conductance was estimated from the amplitude(s) of the open large-conductance channel(s) during a voltage ramp

(from −100 to +100 mV; 1 s duration). Both methods were in excellent agreement when tested on the same patch. BK channels were identified by their characteristic gating behaviour and by exhibiting conductances between 220 and 250 pS as reported by other groups (Latorre *et al.* 1989).

Activating $\alpha5\beta1$ integrin while recording single-channel current proved to be somewhat difficult. We were unable to reliably form outside-out patches that would have permitted bath application of integrin ligands to the exterior surface of excised patches. However, it was possible to maintain cell-attached and inside-out patch recordings when the pipette was dipped in normal pipette solution to fill the tip for a distance of $< 100\ \mu$m, followed by back-filling with the same solution containing soluble FN. Under these recording conditions, diffusion of FN to the tip required 3–5 min, as assessed from pilot experiments using amphotericin B (commonly used for perforated patch recordings) in place of FN and by monitoring the time from initial gigaseal formation to the start of patch permeabilization. The same pipette-filling procedure allowed 3–5 min for the recording of control

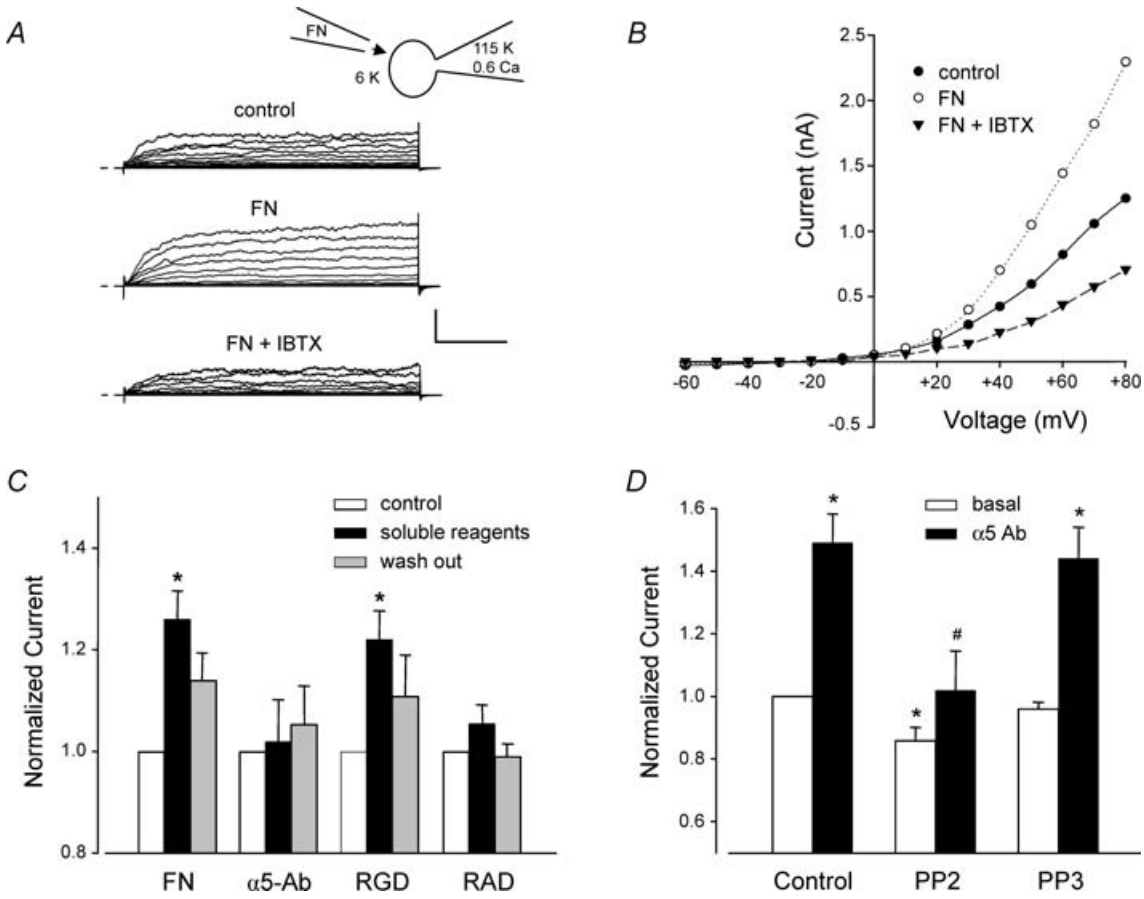

Figure 2. Effects of different $\alpha5\beta1$ integrin ligands on whole-cell VSM K^+ current
A, representative recordings of whole-cell K^+ currents before (control), 3 min after application of soluble FN (10 μg ml^{-1}), and after subsequent addition of IBTX (100 nM) to the bath. Calibration bar: 500 pA, 50 ms. Inset shows recording configuration for all panels. $V_h = -70$ mV. *B*, *I–V* curves derived from current tracings shown in panel *A*. *C*, summary of peak K^+ currents in response to a +50 mV voltage step in which the cells were treated with the following agents for 4 min: soluble FN fragment (10 μg ml^{-1}), soluble RGD peptide (100 μM), soluble $\alpha5$ integrin Ab (15 μg ml^{-1}), or soluble RAD (control peptide for RGD, 100 μM). $^*P < 0.05$ *versus* control. *D*, the soluble c-Src inhibitor PP2 (100 nM, $n = 8$) significantly blocked the potentiation of K^+ current by insoluble $\alpha5$-integrin Ab (measured at 5 min). Pretreatment of cells with PP2 (100 nM) significantly inhibited basal current and prevented enhancement of current after $\alpha5\beta1$ integrin activation. The inactive analogue PP3 (100 nM, $n = 8$) slightly but not significantly decreased basal BK current and did not significantly alter enhancement of current after $\alpha5\beta1$ integrin activation. All values were normalized to the value of control current at a test potential of +50 mV; $V_h = -60$ mV. For panels *A* and *B*, the bath solution was 140 mM Na^+, 6 mM K^+ + 4-AP (1 mM) + glibenclamide (500 nM); the pipette solution contained 115 mM K^+ and 0.6 μM Ca^{2+}. For panels *C* and *D* the bath solution was 136 Na^+ + 1 mM 4-AP + 500 nM glibenclamide; pipette solution: 115 K^+ with 100 nM Ca^{2+}. $^*P < 0.05$ *versus* control (basal current). #$P < 0.05$ *versus* control $\alpha5$-Ab.

channel activity before FN reached the patch. While this approach enabled us to test the effect of soluble FN, we could not test the effect of insoluble $\alpha5\beta1$ integrin Ab (i.e. on beads) or the effect of soluble $\alpha5\beta1$ integrin Ab crosslinked by an appropriate secondary Ab (Yamada *et al.* 1985; Elemer & Edgington, 1994) as we have previously shown is possible under whole-cell recording conditions (Wu *et al.* 1998).

Figure 3*A* shows data obtained from a cell-attached patch when the pipette was back-filled with FN ($15\,\mu g\,ml^{-1}$). At the top is a diagram of the preparation, illustrating the recording configuration with the cell bathed in 140 mM K^+ solution to zero the membrane potential ($V_h = +80$ mV). Immediately after seal formation (arrowhead in the top trace), basal channel activity was quite low and the infrequent openings shown probably represent a mixture of different K^+ channels. However after ~5 min, the open probability of a large amplitude channel increased dramatically (NP_o increased from 0.0032 to 0.23). The amplitude at +80 mV was consistent with current carried by a BK channel, but to confirm this, voltage ramps were used to estimate single-channel conductance. The lower inset shows an example of two ramps (−100 to +100 mV) applied during the first minute after seal formation and then after a sufficient amount of time for FN to diffuse to the membrane (respective times are indicated by open and closed symbols). At ~1 min, there were no channel openings at negative potentials but at ~5 min of recording, channel activity was evident at all potentials between −75 and +100 mV. The conductance of the larger amplitude openings was estimated to be 228 pS, which is consistent with a BK channel (representative of 4 cells). Figure 3*B* summarizes the NP_o values measured from similar protocols before and after FN ($n = 4$). On average, there was a 17-fold increase in NP_o under these recording conditions. Time controls made in other cells without FN in the pipette showed no significant changes in NP_o over the same time scale (0.077 ± 0.001 and 0.082 ± 0.001, respectively).

Under the experimental conditions used in Fig. 3, activation of $\alpha5\beta1$ integrin on the outer surface of the patch could initiate Ca^{2+} entry through L-type and other Ca^{2+} channels that might subsequently activate BK channels in the vicinity of the Ca^{2+} channel (Wang *et al.* 2005; Balasubramanian *et al.* 2007). However, the data in Figs 1 and 2 suggest that $\alpha5\beta1$ integrin activation can activate BK current under conditions where both voltage and intracellular Ca^{2+} are clamped (i.e. using whole-cell voltage clamp and cell dialysis with Ca^{2+}–EGTA from the pipette). Furthermore, inhibition of the response by PP2 (Fig. 2*D*) suggests that the sensitivity of the channel can be increased at a constant $[Ca^{2+}]_i$ by integrin-induced c-*Src* activity (Ling *et al.* 2000). We attempted to further test this idea by increasing the Ca^{2+} buffering on the internal surface of the cell-attached patch. Arteriolar myocytes were pre-loaded with the fast Ca^{2+} chelator BAPTA-AM ($10\,\mu M$) for 15 min and then superfused with 140 mM K^+ bath solution containing variable amounts of Ca^{2+}. When both bath and pipette solutions were Ca^{2+} free, BK channel openings were extremely rare at any voltage, even in the presence of FN ($n = 5$, data not shown). When the pipette solution was nominally Ca^{2+} free and the bath solution contained 1 mM Ca^{2+}, FN-induced K^+ channel openings were observed only at positive potentials during voltage ramps. With 1 mM $CaCl_2$ in the bath and 0.5 mM $CaCl_2$ in the pipette, BK channel openings were rare under control conditions, but FN diffusion to the pipette tip

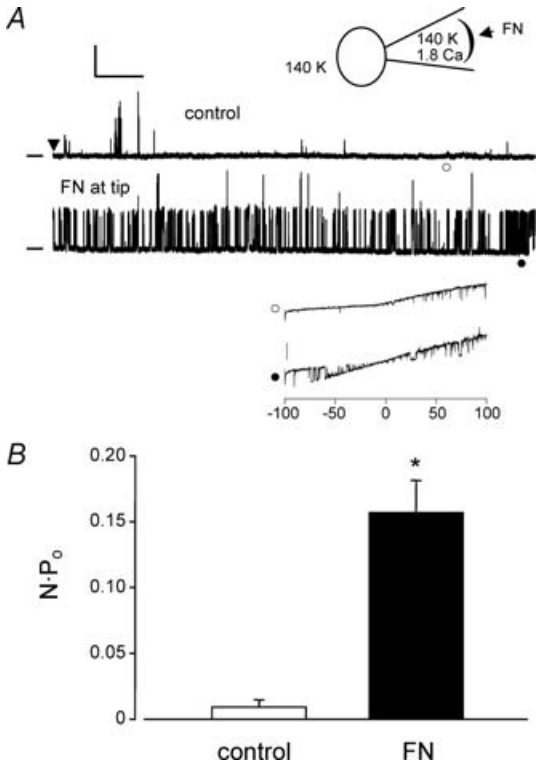

Figure 3. Effect of soluble FN on single-channel BK currents
A, cell-attached patch recording from a VSM cell bathed in solution containing 140 mM K^+ and 2 mM Ca^{2+} (represented by inset diagram). Pipette tip was filled for ~100 μm with 140 mM K^+ pipette solution containing 1.8 mM Ca^{2+}, and then back-filled with the same solution containing FN ($10\,\mu g\,ml^{-1}$). After gigaseal formation, single-channel K^+ currents were recorded at $V_h = +80$ mV. After allowing 5 min for diffusion of FN to the membrane, there was a dramatic increase in the activity of a large-conductance channel (lower trace), with NP_o increasing from 0.0032 to 0.23 in this patch. Calibration bar: 20 pA, 0.5 s. Zero current level is indicated by dash at left. Inset shows current recordings in response to two voltage ramps (from −100 to +100 mV, 1 s duration) performed at 1 min (○) and 5 min (●). Transient openings of a large-conductance K^+ channel were seen first only at positive voltages, but at 5 min, numerous channel openings were evident at both positive and negative voltage potentials. Calibration bar: 20 pA. Conductance of the channel was estimated to be 228 pS (from the lower *I–V* trace). *B*, graph of NP_o (mean ± S.E.M.) at +80 mV before and after FN diffusion to the cell surface ($n = 4$).

(3–5 min after gigaseal formation) induced the opening of a large-conductance channel at both negative and positive potentials. Figure 4*A* shows a recording of K^+ channel activity under the latter conditions, with the membrane potential held at +70 mV. For the first 4 min after gigaseal formation (denoted by the arrowhead in the top trace), very little channel activity was present. At ∼5 min, there was an abrupt opening of a much larger conductance K^+ channel with gating behaviour characteristic of a BK channel (the lower trace shows an expanded time scale). NP_o in this patch increased from 0.00026 (at 1 min) to 0.43 (at 5 min). After the channel opened, current was recorded at various holding potentials to determine channel conductance (not shown), and a conductance estimate of 242 pS was also made using a voltage ramp in the same patch. Figure 4*B* shows the single-channel *I–V* curve averaged from similar recordings made in two cells in which conductance averaged 230 pS. Figure 4*C* summarizes the change in NP_o for three cells under these conditions, where NP_o increased > 400-fold in response to FN. The large relative change in NP_o in Fig. 4*C* compared to that in Fig. 3 was due primarily to a lower basal NP_o caused by the increased Ca^{2+} buffering. The observation that no BK channel activity could be recorded under more stringent Ca^{2+} buffering conditions is consistent with a certain amount of external Ca^{2+} being permissive for increased BK channel activity in response to FN.

While the single-channel recordings in Figs 3 and 4 suggest that BK channels can be activated through a membrane-delimited signalling pathway following $\alpha5\beta1$ integrin engagement, a more definitive test would be to perform similar protocols in excised, inside-out (cell-free) patches. Figure 5 shows the results of such experiments. In Fig. 5*A*, a patch was excised from an arteriolar myocyte and bathed in 140 mM K^+ bath solution at a fixed internal [Ca^{2+}] of 0.8 μM. The pipette solution contained 140 mM K^+ and 1.8 mM Ca^{2+}. To minimize the potential contribution of other K^+ channels, the pipette also included 50 nM apamin (to block small-conductance, Ca^{2+}-activated K^+ channels) and

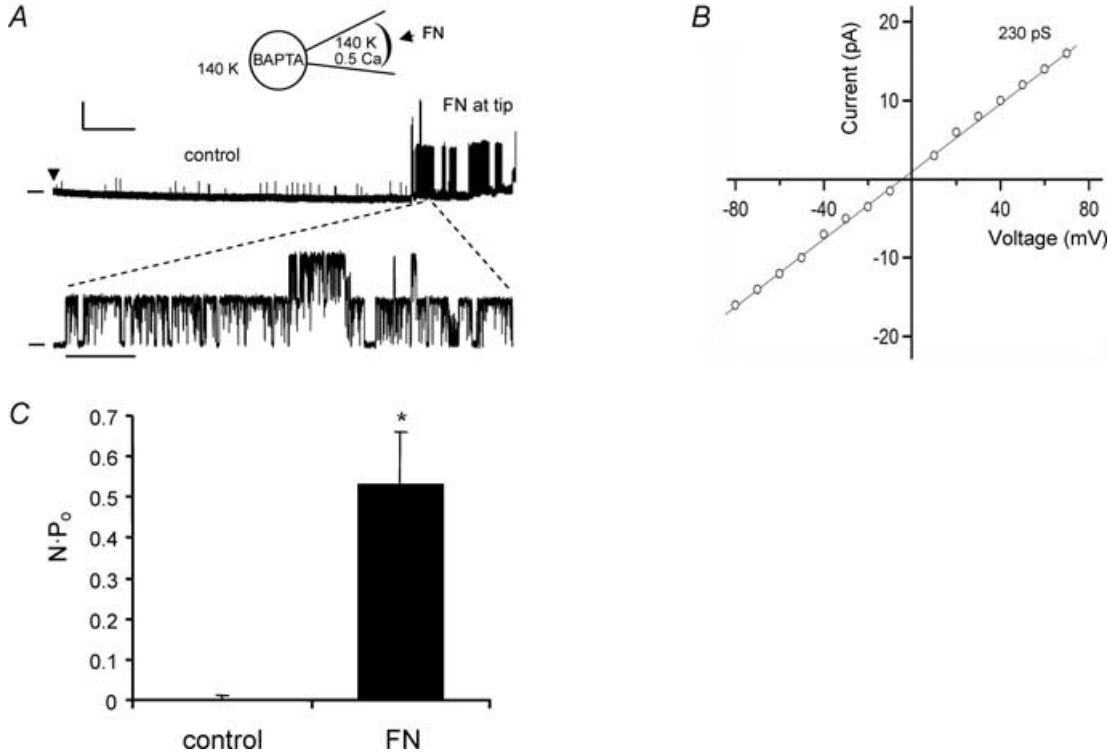

Figure 4. Effect of FN on single-channel BK currents in cells loaded with BAPTA
A, current recording from a cell-attached patch held at $V_h = +70$ mV with cell in 140 K^+ bath solution containing 1 mM Ca^{2+} (depicted by inset diagram). Cell was pre-loaded with BAPTA-AM (10 μM) for 15 min. The patch pipette tip was dipped into 140 K^+ pipette solution containing 0.5 mM Ca^{2+}, 50 nM apamin and 1 μM TRAM-34, then back-filled with the same solution containing FN (10 μg ml^{-1}). Calibration bar: 10 pA, 50 s. An expanded trace is shown in the lower panel, with at least 2 large-conductance channels evident. Time calibration bar: 1 s. Zero current level is indicated by dash at left. *B*, average *I–V* plot obtained from experiments similar to panel *A* with current amplitude measured ∼5 min after gigaseal formation at various holding potentials from −80 mV to +80 mV. The mean slope conductance of the channel was 230 pS ($n = 2$). *C*, average NP_o (mean ± S.E.M.) at +80 mV measured during the first (control) and fifth (FN) minutes using the same protocol as in panel *A*.

1 μM TRAM-34 (to block intermediate-conductance, Ca^{2+}-activated K^+ channels). FN was applied to the cell through the recording pipette as described for Figs 3 and 4. The top trace in Fig. 5*A* shows the baseline channel activity of an inside-out patch during the first minute following patch excision; NP_o was 0.091. The lower trace shows channel activity after ~5 min, allowing for FN to diffuse to the membrane; NP_o had increased to 0.3. Voltage steps were subsequently used to determine the *I–V* relationship for the channel, as shown in Fig. 5*B*. Conductance was 245 pS during the first minute and 255 pS during the fifth minute, consistent with the known behaviour of BK channels in symmetrical high K^+ solutions.

The increase in BK channel activity induced by FN under conditions when membrane potential and intracellular $[Ca^{2+}]$ were fixed is consistent with another mechanism regulating the channel. Subsequently, we tested whether c-Src was involved. Figure 5*C* shows a diagram of the preparation and a sample current recording. A patch was excised from an arteriolar myocyte and exposed to the same solutions as described in Fig. 5*A*. The baseline activity of a large-conductance channel was relatively low for the first few minutes, but increased at about the fifth minute. The inset shows two voltage ramps performed at the times indicated by the open and closed circles. The conductance for the larger unitary current amplitude

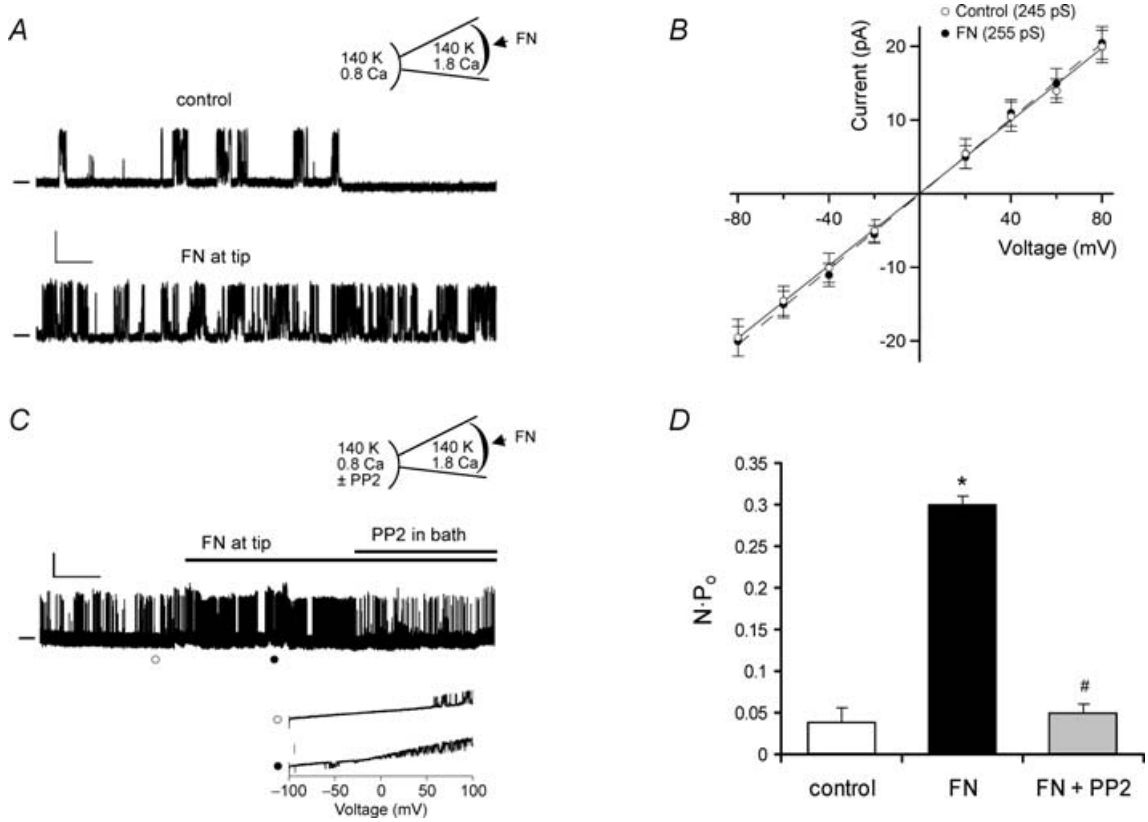

Figure 5. Effect of FN on single-channel BK currents in excised patches
A, current recording from an excised, inside-out patch at $V_h = +60$ mV with patch bathed in 140 K^+ bath solution containing 0.8 μM Ca^{2+} (represented by inset diagram). Pipette tip was filled for ~100 μm with 140 K^+ pipette solution containing 1.8 mM Ca^{2+}, 50 nM apamin, 1 μM TRAM-34 and then back-filled with the same solution containing FN (10 μg ml^{-1}). The upper trace (control) was acquired during the first min after gigaseal formation and the lower trace was acquired after ~5 min, allowing FN time to diffuse to the membrane. Calibration bar: 10 pA, 0.5 s. Zero current level is indicated by dash at left. *B*, *I–V* plot from single-channel currents obtained using same protocol as in panel *A* with current amplitudes measured at ~1 min and ~5 min after gigaseal formation at various holding potentials between −80 mV and +80 mV. *C*, current recording from an excised, inside-out patch at $V_h = +60$ mV with solutions as depicted in inset diagram. PP2 (1 μM) was added to the bath at ~5 min. Calibration bar: 10 pA, 1 min. Inset shows current recordings in response to two voltage ramps (from −100 to +100 mV, 1 s duration) performed at times indicated by ○ (upper trace) and ● (lower trace). Calibration bar for inset: 20 pA. Conductance of the channel in this patch was estimated to be 233 pS from the lower trace. *D*, summary data for NP_o measurements (mean ± S.E.M.) at +80 mV during control, FN, and FN + PP2 periods. The average conductance was 242 ± 5 pS for control; 237 ± 4 pS for FN and 238 ± 5 pS for FN + PP2, as estimated from voltage ramps as shown in *C*. For PP3 experiments using the same protocol, the values of NP_o were 0.04 ± 0.02 for control, 0.48 ± 0.06 for FN, 0.49 ± 0.07 for FN + PP3. $^*P < 0.05$ *versus* control. #$P < 0.05$ *versus* FN.

was 243 pS for control and 235 pS for FN. After channel activity had stabilized at a higher level, PP2 (1 μM) was added to the bath. In the presence of PP2, NP_o rapidly returned toward control levels. Figure 5*D* summarizes the changes in NP_o for this protocol ($n = 4$). On average, FN induced ~8-fold increase in NP_o and the potentiation of channel activity was almost completely reversed by PP2. The inactive analogue PP3 was without significant effect at the same concentration.

Integrin activation enhances activity of heterologously expressed BK channels

VSM cells contain a mixture of different K^+ channels whose activity might be altered directly or indirectly following integrin activation. Although the component of K^+ current potentiated by $\alpha5\beta1$ integrin activation was almost completely eliminated by the selective BK channel toxin inhibitor IBTX (Fig. 1) and single-channel currents activated by FN application had conductances consistent with those of BK channels (Figs 3–5), we sought to confirm our findings in a heterologous cell system that did not endogenously express BK channels. To do this, the pore-forming α-subunit of the mouse BK channel (m*Slo*) was transiently expressed in HEK 293 cells at low density so that whole-cell currents could be recorded without saturating the patch clamp amplifier. Parallel experiments using excised macropatch recordings at higher channel density were conducted in a separate study (Yang *et al.* 2008).

Figure 6*A* shows examples of whole-cell, K^+ current recordings in a non-transfected HEK cell, a cell transfected

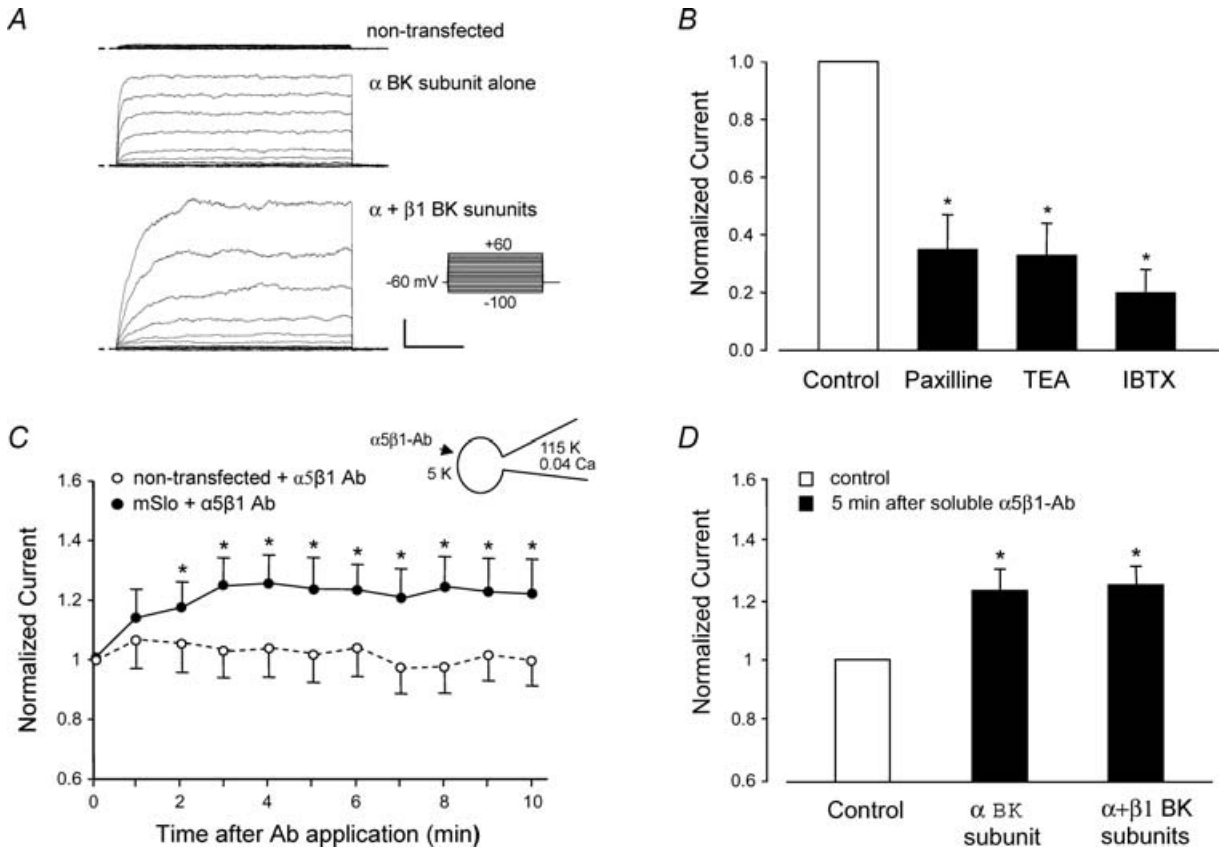

Figure 6. Activation of $\alpha5\beta1$ integrin increases current in heterologously expressed BK channels (m*Slo*)
A, whole-cell currents recorded from HEK 293 cells transiently transfected with cDNA for the murine brain BK α-subunit (m*Slo*). Top trace shows background current level in a representative non-transfected cell; middle trace shows current in cell expressing m*Slo* alone; lower trace shows current in cell expressing both m*Slo* and $\beta1$ BK channel subunits. Calibration bar: 500 pA, 50 ms. *B*, effects on peak m*Slo* currents (at +50 mV) of the BK channel inhibitors paxilline (10 μM), TEA (1 mM), or IBTX (100 nM) added to the bath. *C*, the time course of whole-cell m*Slo* current potentiation after application of soluble $\alpha5\beta1$ integrin Ab (JBS5, 15 μg ml^{-1}) to non-transfected ($n = 7$) or transfected HEK cells (BK α-subunit only, $n = 5$). The enhancement of m*Slo* current at +50 mV was first significant at 2 min and lasted > 10 min. The application of a soluble control Ab (IgG) did not produce a significant change in BK current (not shown). *D*, potentiation of m*Slo* current by $\alpha5\beta1$ integrin Ab in cells expressing m*Slo* alone ($n = 5$) or m*Slo* + $\beta1$ BK subunit ($n = 8$). Inset diagram in *C* shows recording configuration for all panels: whole-cell recording mode, $V_h = -60$ mV; bath solution: 136 mM Na^+; pipette solution: 115 mM K^+ and ~40 nM [Ca^{2+}].

with m*Slo* alone, and a cell transfected with both m*Slo* and $\beta1$ BK channel subunits. The common stimulation protocol is shown at the right. Non-transfected cells exhibited negligible outward current. m*Slo*-transfected cells showed a rapidly activating, non-inactivating outward K^+ current. Cells transfected with both BK channel subunits showed, on average, larger currents and that activated more slowly. These characteristics of heterologously expressed BK channels are in agreement with previous reports from other labs (McManus *et al.* 1995; Nimigean & Magleby, 1999; Cox & Aldrich, 2000). Figure 6*B* shows normalized whole-cell m*Slo* currents recorded before and after addition of the BK channel inhibitors paxilline (100 nM), TEA (1 mM) or IBTX (100 nM) to the bath, confirming that m*Slo* currents were sensitive to classic BK channel inhibitors.

We then tested whether m*Slo* current was potentiated by activation of $\alpha5\beta1$ integrin. HEK cells endogenously express $\alpha5\beta1$ integrin (Yang *et al.* 2008). Although soluble Ab does not activate this integrin in freshly isolated VSM cells (Fig. 2*C*), it does activate the integrin in HEK 293 cells (tSA 201 line), as previously reported (Gui *et al.* 2006), presumably due to the presence of the T surface antigen (and possible integrin crosslinking) in this transformed cell line. Using the whole-cell recording mode, soluble $\alpha5\beta1$ integrin antibody was applied to the cell from the bath. Figure 6*C* plots the time course of whole-cell m*Slo* current following application of soluble $\alpha5\beta1$ integrin Ab (JBS5, 15 μg ml^{-1}). Under these conditions, there was an ~25% increase in outward current in m*Slo*-transfected cells after $\alpha5\beta1$-Ab application, but no significant current increase in non-transfected cells. Furthermore, potentiation followed a time course similar to that of BK current potentiation in native VSM cells after $\alpha5\beta1$ integrin activation (Fig. 1*B*). A similar degree of whole-cell BK current potentiation was observed in cells transfected with both α and $\beta1$ BK channel subunits (Fig. 6*D*), indicating that only the α-subunit was essential for mediating the effect of integrin activation.

Discussion

Our results show that the activation of $\alpha5\beta1$ integrin on the surface of rat arteriolar smooth muscle cells leads to potentiation of BK channel activity through both a Ca^{2+}-dependent mechanism and a phosphorylation mechanism involving c-*Src*. In whole-cell recordings, ligation and clustering of $\alpha5\beta1$ integrin by insoluble $\alpha5\beta1$ antibody (Ab) resulted in ~30–50% increase in BK current amplitude, with the effect first being significant at 1 min and reaching a maximum at 4–5 min. Current potentiation was blocked by the BK channel inhibitor IBTX or by the c-*Src* inhibitor PP2. Soluble FN and RGD peptide each had effects qualitatively similar to insoluble $\alpha5\beta1$ antibody. In cell-attached and inside-out patches, application of the endogenous $\alpha5\beta1$ integrin ligand FN locally to the patch exterior led to large increases in the NP_o of single BK channels, suggesting that the signalling mechanism between the integrin and the channel occurred through a membrane-delimited pathway. Similarly, the enhancement in BK channel activity induced by FN was observed under conditions where intracellular Ca^{2+} was clamped, suggesting that at least part of the effect of integrin activation was mediated by an increase in BK channel Ca^{2+} sensitivity. The effects of $\alpha5\beta1$ integrin activation on BK current could be reproduced in HEK 293 cells expressing the BK channel α-subunit. These findings are consistent with previous observations that the vasodilatory effects of RGD peptide on rat skeletal muscle arterioles (Platts *et al.* 1998) were mediated by the activation of one or more K^+ channels. Our results show that ECM–integrin interactions can regulate VSM BK channels suggesting that this mechanism may play a role in the control of blood flow under both physiological and pathological conditions (Zhou *et al.* 2005).

Coordinated regulation of BK and Ca^{2+} channels by $\alpha5\beta1$ integrin

Previous work from our laboratory demonstrated that ligands of $\alpha5\beta1$ integrin (the FN receptor) and $\alpha v\beta3$ integrin (the vitronectin receptor) reciprocally regulate L-type Ca^{2+} current in myocytes isolated from rat skeletal muscle arterioles (Wu *et al.* 1998). Activation of $\alpha5\beta1$ integrin can evoke an ~70% increase in whole-cell L-type Ca^{2+} current in VSM (Wu *et al.* 2001) and > 2-fold change in whole-cell Cav1.2 current in HEK 293 cells heterologously expressing Cav1.2 channels (Gui *et al.* 2006). Integrin-induced potentiation of Cav1.2 current is mediated by phosphorylation of the channel α-subunit on two C-terminal residues by PKA and c-*Src*. Our finding in the present study that the soluble c-*Src* inhibitor, PP2, blocked BK current potentiation following $\alpha5\beta1$ integrin activation implies that c-*Src* is a key downstream mediator of integrin signalling to both channels. The specific role of c-*Src* in BK channel regulation under these conditions is the topic of a separate study (Yang *et al.* 2008). The activation of a channel that promotes vasodilatation (BK) and a channel that promotes vasoconstriction (Cav1.2) would seemingly lead to antagonistic effects on vascular tone. However, the time courses for integrin-induced potentiation of current in the two channels are different, with potentiation of BK channels being slightly delayed but more sustained (Fig. 1) relative to the potentiation of Cav1.2 channels (Wu *et al.* 1998). Therefore, the net effect of $\alpha5\beta1$ integrin activation in VSM would be a transient

increase in Ca^{2+} influx that is attenuated or terminated by BK-induced membrane hyperpolarization. Presumably, this influx subsequently triggers Ca^{2+} release and/or Ca^{2+}-dependent intracellular signalling mechanisms.

Integrin-induced membrane hyperpolarization has been reported in other cell types (Arcangeli *et al.* 1987, 1989; Hofmann *et al.* 2001), but our results provide the first evidence that BK channel activation may be a key underlying mechanism in VSM. Arcangeli and colleagues first reported that FN–integrin interactions elicited hyperpolarization of murine erythroleukaemia cells (Arcangeli *et al.* 1991), an effect presumably mediated by the activation of Ca^{2+}-activated K^+ channels (Arcangeli *et al.* 1987, 1989). The same group has also shown that the activation of $\beta1$ integrins in neuroblastoma and haemopoietic tumour cells leads to sustained activation of hERG K^+ current (Hofmann *et al.* 2001). $\alpha v\beta3$ integrin activation by vitronectin in cultured endothelial cells also induces membrane hyperpolarization mediated by outward BK current (Kawasaki *et al.* 2004). That result is consistent with, but not necessarily linked to, the observation that the $\alpha v\beta3$ integrin-blocking Ab, F11, prevents (attenuates) flow-induced dilatation of arterioles (Muller *et al.* 1997), a response known to be associated with K^+ channel activation (Platts *et al.* 1998).

Using single-channel recording methods in the present study, we were able to demonstrate that BK channel activity was potentiated as a consequence of integrin activation. We sought to answer at least two questions with single channel experiments: (1) Is the signalling between $\alpha5\beta1$ integrin and the BK channel membrane delimited, i.e. is the entire complement of signalling machinery contained within the patch? (2) Is the increase in channel activity explained simply by an increase in global/local $[Ca^{2+}]$ as a result of integrin-mediated Ca^{2+} entry or release, or is there also a shift in BK channel sensitivity to a given concentration of intracellular Ca^{2+}? The latter mechanism would implicate a possible channel phosphorylation mechanism, which has previously been shown to modify Ca^{2+} sensitivity of the BK channel (Reinhart *et al.* 1991; Taniguchi *et al.* 1993; Ling *et al.* 2000; Alioua *et al.* 2002). In single-channel recordings, the activation of BK channels could possibly be obscured by the presence of other native K^+, Cl^- and/or cation channels, especially in the absence of compounds to specifically block them. Indeed, we routinely observed the activity of outward currents through channels of various conductances under basal conditions (see Figs 3–5). For this reason, it was important to verify the single-channel conductance of any putative BK channel for which gating appeared to be increased in association with FN application; in each recording considered for further analysis, the conductance was well within the range previously reported for BK channels (Figs 3–5).

In cell-attached patches, BK channel activity was significantly increased after localized application of FN to the patch exterior via the recording pipette. To detect the effects of FN against a background of basal BK channel activity, which could vary widely from patch to patch, the pipette tip was filled with FN-free solution, while the remainder of the pipette was back-filled with FN-containing solution. Adjusting the amount of tip filling gave variable amounts of time for 'control' recordings before FN diffused to the surface of the patch. FN-induced BK channel gating in this protocol demonstrates that all of the enzymatic machinery for channel activation is contained in the vicinity of the membrane patch where BK channel activity was measured. However, intracellular $[Ca^{2+}]$ was, again, not controlled and the increase in BK channel activity could have reflected a local change in Ca^{2+} due to FN-stimulated Ca^{2+} entry/release within the patch environment. When local Ca^{2+} changes were minimized by pre-loading the cells with the fast Ca^{2+} chelator BAPTA, a large increase in BK channel activity still occurred in response to patch-specific FN application. The left-ward shift in the *I–V* relationship was suggestive of an increase in Ca^{2+} sensitivity, although we had no way to verify the extent to which intracellular $[Ca^{2+}]$ remained constant. It is interesting to note, however, that a minimal level of Ca^{2+} was needed in the recording pipette under such conditions to even record basal channel activity. The strongest evidence for integrin-induced BK channel potentiation being at least partially mediated by a shift in Ca^{2+} sensitivity came from excised, inside-out patch recordings, where $[Ca^{2+}]$ on the inner surface of the patch remained fixed while FN was applied to the outer surface of the patch through the recording pipette. Under those conditions, integrin-induced potentiation of BK channel activity was still consistently observed (Figs 4 and 5), but at a lower $[Ca^{2+}]$ than reported by Ling (Ling *et al.* 2000), possibly due to the presence of the $\beta1$ BK channel subunit in native VSM cells that would enhance the Ca^{2+} sensitivity of the channel. Furthermore, the effect of FN in the same recording configuration was almost completely blocked by PP2 (Fig. 5). The effect of $\alpha5\beta1$ integrin activation on BK channel Ca^{2+} sensitivity, and the role of c-Src in that process, are issues that are explored in more detail in a separate study (Yang *et al.* 2008).

It is interesting that FN produced, on average, a 26% increase in whole-cell BK current (Fig. 2*A*), but produced much larger (10- to 20-fold) increases in BK single channel activity (quantified as NP_o in excised patches) (Figs 3*B* and 5*D*). There are a number of likely explanations for this apparent discrepancy. First, cytosolic free Ca^{2+} was held at a higher concentration in excised patch *versus* whole-cell recordings – a condition under which integrin activation would be expected to lead to a larger increase in the activity of single-channel events (Yang *et al.* 2008). Second, one would expect that the single-channel data

shown here represent only a subset of the response of the entire BK channel population in a given cell in which FN was observed to have an effect. Since we had no independent method of verifying whether FN reached the extracellular surface of every membrane patch tested, we were able to quantify the effect of FN *only* in patches where (1) BK channels were observed to be present before FN application (Fig. 5*A*) or (2) FN stimulated BK channel activity in the absence of basal channel activity (Fig. 4*A*). In fact, we observed no response to FN in about 40% of total patches examined and therefore did not include those cells in the NP_o analysis. Thus, the single-channel recordings shown here only illustrate the effect of FN on a portion of BK channels in a single cell, such that any recorded macroscopic whole-cell current will reflect a mixed population of stimulated and unstimulated BK channels. If colocalization of the channel and integrin is necessary for channel modulation, some channels would predictably be unaffected by FN–integrin binding, since it is unlikely that all BK channels in a given smooth muscle cell colocalize with $\alpha5\beta1$ integrin. Despite these caveats, our experiments demonstrate that all of the functional signalling components between the $\alpha5\beta1$ integrin and the BK channel are contained within the patch and that the increase in channel activity is mediated in part by a shift in Ca^{2+} sensitivity, due to the activity of c-*Src*.

Physiological relevance of BK channel regulation by ECM

The blood vessel wall is composed of a number of different extracellular matrix proteins, including collagen, fibronectin and laminin (Weber & McFadden, 1997; Bonacci *et al.* 2006; Lebleu *et al.* 2007). Matrix composition is reported to change as the vessel wall is remodelled in disease states such as hypertension, diabetes, ischaemia-reperfusion injury and atherosclerosis (Cagliero *et al.* 1988; Roth *et al.* 1993; Bezie *et al.* 1998; Brownlee, 2000; Intengan & Schiffrin, 2000). For example, osteopontin, fibrinogen and vitronectin – ECM proteins not normally found in the vessel wall at significant levels – are deposited during the formation of an atherosclerotic plaque. With wall remodelling, there are also corresponding changes in both the number and type of integrins expressed by VSM and endothelium (Roth *et al.* 1993; Regoli & Bendayan, 1997; Intengan *et al.* 1999). These changes in wall composition occur in parallel with impaired vascular reactivity (Hultgardh-Nilsson & Durbeej, 2007; Strom *et al.* 2007).

A possible explanation for changes in vascular reactivity under these conditions involves alterations in the signalling between adhesion molecules and vascular ion channels. Indeed, a number of studies have now shown that integrin ligands can acutely regulate the tone of blood vessels (Mogford *et al.* 1997; Muller *et al.* 1997; Platts *et al.* 1998), in part through the role that integrins play in mechanotransduction (Martinez-Lemus *et al.* 2005; Heerkens *et al.* 2007; Lal *et al.* 2007). In addition, matrix degradation subsequent to chronic remodelling, inflammation and vascular wall injury results in the release of cryptic matrix fragments (matricryptins), some of which are vasoactive (Mogford *et al.* 1997; Bayless *et al.* 2000; Davis *et al.* 2000). In this context, $\alpha v\beta3$ integrin has been proposed to function as an injury receptor that may detect the presence of proteins such as vitronectin and osteopontin (Davis *et al.* 2000). Vitronectin is known to activate BK current through $\alpha v\beta3$ integrin in vascular endothelium (Kawasaki *et al.* 2004). Therefore, it is reasonable to expect that changes in the vascular ECM-integrin composition, and the consequent changes in the signalling pathways downstream from those integrins, including BK channel activation, underlie part of the altered vascular reactivity associated with many vascular diseases.

References

Akbarali HI, Thatte H, He XD, Giles WR & Goyal RK (1999). Role of HERG-like K^+ currents in opossum esophageal circular smooth muscle. *Am J Physiol Cell Physiol* **277**, C1284–C1290.

Alioua A, Mahajan A, Nishimaru K, Zarei MM, Stefani E & Toro L (2002). Coupling of c-Src to large conductance voltage- and Ca^{2+}-activated K^+ channels as a new mechanism of agonist-induced vasoconstriction. *Proc Natl Acad Sci U S A* **99**, 14560–14565.

Arcangeli A, Becchetti A, Del Bene MR, Wanke E & Olivotto M (1991). Fibronectin-integrin binding promotes hyperpolarization of murine erythroleukemia cells. *Biochem Biophys Res Commun* **177**, 1266–1272.

Arcangeli A, Becchetti A, Mannini A, Mugnai G, De Filippi P, Tarone G, Del Bene MR, Barletta E, Wanke E & Olivotto M (1993). Integrin-mediated neurite outgrowth in neuroblastoma cells depends on the activation of potassium channels. *J Cell Biol* **122**, 1131–1143.

Arcangeli A, Riccarda Del Bene M, Poli R, Ricupero L & Olivotto M (1989). Mutual contact of murine erythroleukemia cells activates depolarizing cation channels, whereas contact with extracellular substrata activates hyperpolarizing Ca^{2+}-dependent K^+ channels. *J Cell Physiol* **139**, 1–8.

Arcangeli A, Wanke E, Olivotto M, Camagni S & Ferroni A (1987). Three types of ion channels are present on the plasma membrane of Friend erythroleukemia cells. *Biochem Biophys Res Commun* **146**, 1450–1457.

Balasubramanian L, Ahmed A, Lo CM, Sham JS & Yip KP (2007). Integrin-mediated mechanotransduction in renal vascular smooth muscle cells: activation of calcium sparks. *Am J Physiol Regul Integr Comp Physiol* **293**, R1586–R1594.

Bayless KJ, Salazar R & Davis GE (2000). RGD-dependent vacuolation and lumen formation observed during endothelial cell morphogenesis in three-dimensional fibrin matrices involves the $\alpha_v\beta_3$ and $\alpha_5\beta_1$ integrins. *Am J Pathol* **156**, 1673–1683.

Becchetti A, Arcangeli A, Del Bene MR, Olivotto M & Wanke E (1992). Response to fibronectin–integrin interaction in leukaemia cells: delayed enhancing of a K^+ current. *Proc Biol Sci* **248**, 235–240.

Bezie Y, Lamaziere JM, Laurent S, Challande P, Cunha RS, Bonnet J & Lacolley P (1998). Fibronectin expression and aortic wall elastic modulus in spontaneously hypertensive rats. *Arterioscler Thromb Vasc Biol* **18**, 1027–1034.

Bonacci JV, Schuliga M, Harris T & Stewart AG (2006). Collagen impairs glucocorticoid actions in airway smooth muscle through integrin signalling. *Br J Pharmacol* **149**, 365–373.

Braun AP & Sy L (2001). Contribution of potential EF hand motifs to the calcium-dependent gating of a mouse brain large conductance, calcium-sensitive K^+ channel. *J Physiol* **533**, 681–695.

Brayden JE & Nelson MT (1992). Regulation of arterial tone by activation of calcium-dependent potassium channels. *Science* **256**, 532–535.

Brenner R, Perez GJ, Bonev AD, Eckman DM, Kosek JC, Wiler SW, Patterson AJ, Nelson MT & Aldrich RW (2000). Vasoregulation by the $\beta 1$ subunit of the calcium-activated potassium channel. *Nature* **407**, 870–876.

Brownlee M (2000). Negative consequences of glycation. *Metabolism* **49**, 9–13.

Cagliero E, Maiello M, Boeri D, Roy S & Lorenzi M (1988). Increased expression of basement membrane components in human endothelial cells cultured in high glucose. *J Clin Invest* **82**, 735–738.

Clark EA & Brugge JS (1995). Integrins and signal transduction pathways: the road taken. *Science* **268**, 233–239.

Cox DH & Aldrich RW (2000). Role of the $\beta 1$ subunit in large-conductance Ca^{2+}-activated K^+ channel gating energetics. Mechanisms of enhanced Ca^{2+} sensitivity. *J Gen Physiol* **116**, 411–432.

Davis GE, Bayless KJ, Davis MJ & Meininger GA (2000). Regulation of tissue injury responses by the exposure of matricryptic sites within extracellular matrix molecules. *Am J Pathol* **156**, 1489–1498.

Davis MJ, Wu X, Nurkiewicz TR, Kawasaki J, Davis GE, Hill MA & Meininger GA (2001). Integrins and mechanotransduction of the vascular myogenic response. *Am J Physiol Heart Circ Physiol* **280**, H1427–H1433.

Davis MJ, Wu X, Nurkiewicz TR, Kawasaki J, Gui P, Hill MA & Wilson E (2002). Regulation of ion channels by integrins. *Cell Biochem Biophys* **36**, 41–66.

Elemer GS & Edgington TS (1994). Two independent sets of monoclonal antibodies define neoepitopes linked to soluble ligand binding and leukocyte adhesion functions of activated αM $\beta 2$. *Circ Res* **75**, 165–171.

Gui P, Wu X, Ling S, Stotz SC, Winkfein RJ, Wilson E, Davis GE, Braun AP, Zamponi GW & Davis MJ (2006). Integrin receptor activation triggers converging regulation of Cav1.2 calcium channels by c-Src and protein kinase A pathways. *J Biol Chem* **281**, 14015–14025.

Hamill OP, Marty A, Neher E, Sakmann B & Sigworth FJ (1981). Improved patch-clamp techniques for high-resolution current recording from cells and cell-free membrane patches. *Pflugers Arch* **391**, 85–100.

Heerkens EH, Izzard AS & Heagerty AM (2007). Integrins, vascular remodeling, and hypertension. *Hypertension* **49**, 1–4.

Hofmann G, Bernabei PA, Crociani O, Cherubini A, Guasti L, Pillozzi S, Lastraioli E, Polvani S, Bartolozzi B, Solazzo V, Gragnani L, Defilippi P, Rosati B, Wanke E, Olivotto M & Arcangeli A (2001). HERG K^+ channels activation during B_1 integrin-mediated adhesion to fibronectin induces an up-regulation of $\alpha_v\beta_3$ integrin in the preosteoclastic leukemia cell line FLG 29.1. *J Biol Chem* **276**, 4923–4931.

Hultgardh-Nilsson A & Durbeej M (2007). Role of the extracellular matrix and its receptors in smooth muscle cell function: implications in vascular development and disease. *Curr Opin Lipidol* **18**, 540–545.

Intengan HD, Deng LY, Li JS & Schiffrin EL (1999). Mechanics and composition of human subcutaneous resistance arteries in essential hypertension. *Hypertension* **33**, 569–574.

Intengan HD & Schiffrin EL (2000). Structure and mechanical properties of resistance arteries in hypertension: role of adhesion molecules and extracellular matrix determinants. *Hypertension* **36**, 312–318.

Jackson WF & Blair KL (1998). Characterization and function of Ca^{2+}-activated K^+ channels in arteriolar muscle cells. *Am J Physiol Heart Circ Physiol* **274**, H27–H34.

Kawasaki J, Davis GE & Davis MJ (2004). Regulation of Ca^{2+}-dependent K^+ current by $\alpha v\beta 3$ integrin engagement in vascular endothelium. *J Biol Chem* **279**, 12959–12966.

Lal H, Verma SK, Smith M, Guleria RS, Lu G, Foster DM & Dostal DE (2007). Stretch-induced MAP kinase activation in cardiac myocytes: differential regulation through $\beta 1$-integrin and focal adhesion kinase. *J Mol Cell Cardiol* **43**, 137–147.

Latorre R, Oberhauser A, Labarca P & Alvarez O (1989). Varieties of calcium-activated potassium channels. *Annu Rev Physiol* **51**, 385–399.

Lebleu VS, Macdonald B & Kalluri R (2007). Structure and function of basement membranes. *Exp Biol Med (Maywood)* **232**, 1121–1129.

Ling S, Woronuk G, Sy L, Lev S & Braun AP (2000). Enhanced activity of a large conductance, calcium-sensitive K^+ channel in the presence of Src tyrosine kinase. *J Biol Chem* **275**, 30683–30689.

McManus OB, Helms LM, Pallanck L, Ganetzky B, Swanson R & Leonard RJ (1995). Functional role of the β subunit of high conductance calcium-activated potassium channels. *Neuron* **14**, 645–650.

Martinez-Lemus LA, Crow T, Davis MJ & Meininger GA (2005). $\alpha v\beta 3$- and $\alpha 5\beta 1$-integrin blockade inhibits myogenic constriction of skeletal muscle resistance arterioles. *Am J Physiol Heart Circ Physiol* **289**, H322–H329.

Mogford JE, Davis GE & Meininger GA (1997). RGDN peptide interaction with endothelial $\alpha 5\beta 1$ integrin causes sustained endothelin-dependent vasoconstriction of rat skeletal muscle arterioles. *J Clin Invest* **100**, 1647–1653.

Mogford JE, Davis GE, Platts SH & Meininger GA(1996). Vascular smooth muscles $\alpha v\beta 3$ integrin mediates arteriolar vasodilation in response to RGD peptides. *Circ Res* **79**, 821–826.

Muller JM, Chilian WM & Davis MJ (1997). Integrin signaling transduces shear stress-dependent vasodilation of coronary arterioles. *Circ Res* **80**, 320–326.

Nelson MT & Quayle JM (1995). Physiological roles and properties of potassium channels in arterial smooth muscle. *Am J Physiol Cell Physiol* **268**, C799–C822.

Nimigean CM & Magleby KL (1999). The β subunit increases the Ca^{2+} sensitivity of large conductance Ca^{2+}-activated potassium channels by retaining the gating in the bursting states. *J Gen Physiol* **113**, 425–440.

Platts SH, Mogford JE, Davis MJ & Meininger GA (1998). Role of K^+ channels in arteriolar vasodilation mediated by integrin interaction with RGD-containing peptide. *Am J Physiol Heart Circ Physiol* **275**, H1449–H1454.

Regoli M & Bendayan M (1997). Alterations in the expression of the $\alpha3\beta1$ integrin in certain membrane domains of the glomerular epithelial cells (podocytes) in diabetes mellitus. *Diabetologia* **40**, 15–22.

Reinhart PH, Chung S, Martin BL, Brautigan DL & Levitan IB (1991). Modulation of calcium-activated potassium channels from rat brain by protein kinase A and phosphatase 2A. *J Neurosci* **11**, 1627–1635.

Roth T, Podesta F, Stepp MA, Boeri D & Lorenzi M (1993). Integrin overexpression induced by high glucose and by human diabetes: potential pathway to cell dysfunction in diabetic microangiopathy. *Proc Natl Acad Sci U S A* **90**, 9640–9644.

Silletti S, Mei F, Sheppard D & Montgomery AM (2000). Plasmin-sensitive dibasic sequences in the third fibronectin-like domain of L1-cell adhesion molecule (CAM) facilitate homomultimerization and concomitant integrin recruitment. *J Cell Biol* **149**, 1485–1502.

Sohma Y, Harris A, Wardle CJ, Argent BE & Gray MA (1996). Two barium binding sites on a maxi K^+ channel from human vas deferens epithelial cells. *Biophys J* **70**, 1316–1325.

Strom A, Fredrikson GN, Schiopu A, Ljungcrantz I, Soderberg I, Jansson B, Carlsson R, Hultgardh-Nilsson A & Nilsson J (2007). Inhibition of injury-induced arterial remodelling and carotid atherosclerosis by recombinant human antibodies against aldehyde-modified apoB-100. *Atherosclerosis* **190**, 298–305.

Swayze RD & Braun AP (2001). A catalytically inactive mutant of type I cGMP-dependent protein kinase prevents enhancement of large conductance, calcium-sensitive K^+ channels by sodium nitroprusside and cGMP. *J Biol Chem* **276**, 19729–19737.

Taniguchi J, Furukawa KI & Shigekawa M (1993). Maxi K^+ channels are stimulated by cyclic guanosine monophosphate-dependent protein kinase in canine coronary artery smooth muscle cells. *Pflugers Arch* **423**, 167–172.

Toro L, Wallner M, Meera P & Tanaka Y (1998). Maxi-K_{Ca}, a unique member of the voltage-gated K channel superfamily. *News Physiol Sci* **13**, 112–117.

Tsao PW & Mousa SA (1995). Thrombospondin mediates calcium mobilization in fibroblasts via its Arg-Gly-Asp and carboxyl-terminal domains. *J Biol Chem* **270**, 23747–23753.

Wang J, Shimoda LA, Weigand L, Wang W, Sun D & Sylvester JT (2005). Acute hypoxia increases intracellular $[Ca^{2+}]$ in pulmonary arterial smooth muscle by enhancing capacitative Ca^{2+} entry. *Am J Physiol Lung Cell Mol Physiol* **288**, L1059–L1069.

Weber DJ & McFadden PN (1997). Injury-induced enzymatic methylation of aging collagen in the extracellular matrix of blood vessels. *J Protein Chem* **16**, 269–281.

Wu X, Davis GE, Meininger GA, Wilson E & Davis MJ (2001). Regulation of the L-type calcium channel by $\alpha5\beta1$ integrin requires signaling between focal adhesion proteins. *J Biol Chem* **276**, 30285–30292.

Wu X, Mogford JE, Platts SH, Davis GE, Meininger GA & Davis MJ (1998). Modulation of calcium current in arteriolar smooth muscle by $\alpha v\beta3$ and $\alpha5\beta1$ integrin ligands. *J Cell Biol* **143**, 241–252.

Yamada KM, Akiyama SK, Hasegawa T, Hasegawa E, Humphries MJ, Kennedy DW, Nagata K, Urushihara H, Olden K & Chen WT (1985). Recent advances in research on fibronectin and other cell attachment proteins. *J Cell Biochem* **28**, 79–97.

Yang Y, Wu X, Wu JB, Sheng JZ, Ling S, Braun AP, Davis GE & Davis MJ(2008). $\alpha5\alpha1$ integrin activation increases BK channel current and Ca^{2+} sensitivity through c-Src mediated channel phosphorylation. *J Biol Chem*.

Zhou R, Liu L & Hu D (2005). Involvement of BKCa α subunit tyrosine phosphorylation in vascular hyporesponsiveness of superior mesenteric artery following hemorrhagic shock in rats. *Cardiovasc Res* **68**, 327–335.

Acknowledgements

We thank David Durtschi and Judy Davidson for their technical assistance. We are also grateful to Drs David Murchison and William Griffith for advice concerning several of the patch clamp protocols. This work was supported by NIH grants HL-072989 and HL-089784.